ISSN 0030-400X, Optics and Spectroscopy, 2019, Vol. 126, No. 2, pp. 154–160. © Pleiades Publishing, Ltd., 2019.
Russian Text © A.S. Abramov, D.A. Evseev, I.O. Zolotovskii, D.I. Sementsov, 2019, published in Optika i Spektroskopiya, 2019, Vol. 126, No. 2, pp. 224–230.

FIBER OPTICS AND INTEGRATED OPTICS

Dispersion of Bulk Waves in a Graphene–Dielectric–Graphene Structure

A. S. Abramov[a], *, D. A. Evseev[a], I. O. Zolotovskii[a], and D. I. Sementsov[a]

[a] *Ulyanovsk State University, Ulyanovsk, 432970 Russia*

**e-mail: aleksei_abramov@mail.ru*

Received August 15, 2018; revised September 21, 2018

Abstract—We investigate the dispersion properties of the first waveguide modes in a dielectric film that is coated with graphene layers having different chemical potential values. The control over the phase and group velocities of the first waveguide mode is considered. Spectral intervals in which the phase velocity of the waveguide modes is small, while their group velocity is negative, are revealed. We show that the dispersion characteristics of the waveguide modes can be rearranged using an external electric field.

DOI: 10.1134/S0030400X19020024

INTRODUCTION

In recent times, metal–dielectric planar structures, in particular, their waveguide properties, have attracted attention from researchers [1–3]. One such important property of these structures is the occurrence of a broad frequency range in metals in which the dielectric permittivity is negative, which makes it possible to excite surface plasmon polaritons at interfaces between a metal and a dielectric [4]. The wave characteristics of surface and bulk plasmon polaritons are largely determined by the character of the dispersion of material parameters of bordering media. The behavior of plasmon polaritons in metal–dielectric waveguide structures and the possibilities of their practical applications have been considered in detail in [3, 5–7]. However, the use of metal films as a waveguiding layers inevitably leads to significant losses and to a significant decrease in the path length of plasmon polaritons.

Waveguiding structures in which propagating waves can be substantially slowed down are of considerable interest, since this is important for solving many applied problems of photonics. There are many materials and structures in which the propagation of slow waves has been theoretically predicted and experimentally realized. First of all, these are high-temperature superconductors [8], photonic crystals and metamaterials [9], and planar structures containing semiconductor films [10].

Deceleration of waves and control over their dispersion characteristics in guiding structures can also be achieved by forming structures using graphene layers, the chemical potential (ChP) of which significantly depends on the temperature and external electric field [11, 12]. Graphene layers can be used as coatings of a dielectric core in planar waveguides [11, 13–15] or in optical fibers [16], as well as in more complex structures. It was shown in [17] that the dispersion properties of waveguide TE modes in a rectangular waveguide with metal walls, dielectric filling, and a graphene layer can be controlled not only by changing the ChP of the graphene layer, but also by its positioning inside the waveguide. The authors of [18] investigated peculiarities of the dispersion of surface plasmons in a structure formed by a rectangular dielectric waveguide, a graphene monolayer, and a coating medium. Efficient control of the properties of guided waves in various waveguide structures based on graphene can be realized both by electric and by magnetic fields [19].

In this work, we study the effect of graphene layers deposited on the surface of a dielectric film on the dispersion properties of waveguide modes in the film. The possibility of controlling the phase and group velocities of waveguide modes by symmetric or asymmetric changing of the ChP of the graphene layers is considered.

MATERIAL PARAMETERS OF THE STRUCTURE

Let us investigate the waveguide propagation regime of modes in a planar structure that consists of a thin dielectric film with thickness d, dielectric permittivity ε_d of which does not have dispersion in the spectral range under consideration and is a real-valued quantity. On the two surfaces of the film, $z = 0$ and $z = d$, two monolayers of graphene are deposited with different ChPs, μ_1 and μ_2; therefore, the conductivities of the layers, σ_1 and σ_2, are also different. The film with

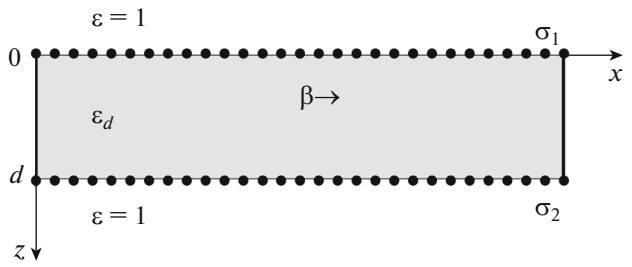

Fig. 1. Geometry of a structure.

the graphene layers is placed between two nonmagnetic media with dielectric permittivities ε_1 and ε_3. The geometry of the structure is shown in Fig. 1.

The frequency dependences of the real and imaginary parts of the complex surface conductivity $\sigma = \sigma' + i\sigma''$ of doped graphene were determined in terms of the Kubo model by the following relationships [20–22]:

$$\frac{\sigma'}{\sigma_0} = \frac{1}{2} + \frac{1}{\pi}\arctan\left(\frac{h\omega - 2\mu}{2k_BT}\right),$$

$$\frac{\sigma''}{\sigma_0} = \frac{1}{2\pi} = \left[\left(\frac{16k_BT}{h\omega}\ln\left(2\cosh\left(\frac{\mu}{2k_BT}\right)\right)\right.\right. \quad (1)$$

$$\left.\left. - \ln\left(\frac{(h\omega + 2\mu)^2}{(h\omega - 2\mu)^2 + (2k_BT)^2}\right)\right)\right].$$

Here, $\sigma_0 = e^2/4h$ is the fundamental (static) conductivity of graphene, e is the electron charge, h is the Planck constant, ω is frequency, k_B is the Boltzmann constant, and T is temperature. The ChP in these expressions is given by $\mu = \hbar v_F\sqrt{\pi n_0}$, where n_0 and v_0 are the concentration of charge carriers and the Fermi velocity in graphene.

Figure 2 shows the frequency dependences of the real and imaginary parts of the surface conductivity of graphene, which were plotted in accordance with expressions (1) for values of the ChP $\mu = -0.1$, 0.0, 0.1, 0.2, and 0.3 eV (curves *1–5*), which can be varied experimentally with an external electric field. Hereinafter, our numerical analysis was carried out at the working temperature of $T = 300$ K. Zero and negative values of the ChP are achieved by applying zero and reverse bias voltages, respectively [23]. It can be seen that, as the ChP increases, the range of growth of intrinsic conductivity σ' shifts to higher frequencies (curves *3–5* in Fig. 2a). The same shift is also experienced by a minimum of the imaginary part of conductivity σ'' (curves *3–5* in Fig. 2b). At zero and negative values of the ChP, the real part of the conductivity is practically independent of frequency (curves *1* and *2* in Fig. 2a), and the imaginary parts do not enter the

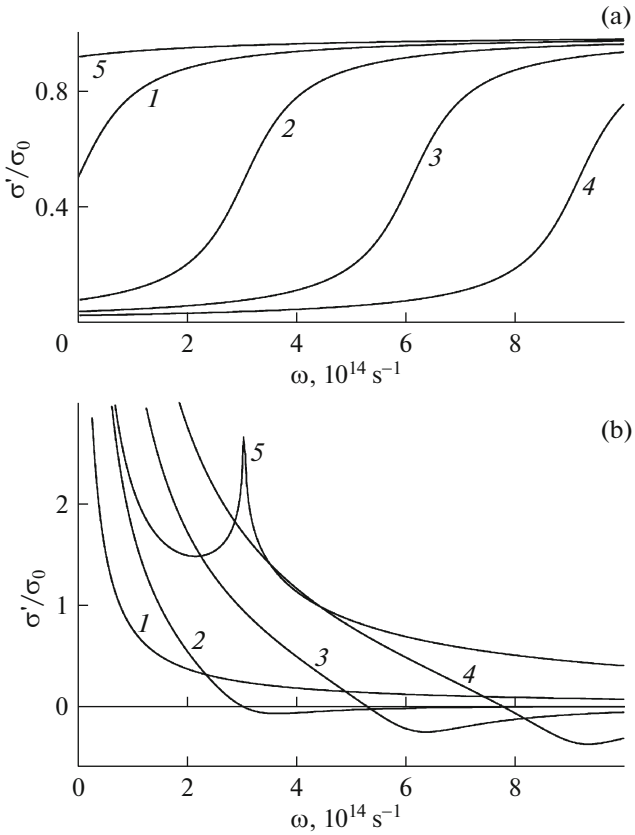

Fig. 2. Frequency dependences of (a) real σ' and (b) imaginary σ'' parts of the surface conductivity of graphene at $\mu = 0$, 0.1, 0.2, 0.3, and –0.1 eV (curves *1–5*).

negative range (curves *1* and *2* in Fig. 2b). If the imaginary part of the conductivity is negative in a fairly wide frequency range (curves *3–5* in Fig. 2b), in a dielectric waveguide with graphene layers on the surfaces, the propagation of both waveguide and surface modes is possible. Under the condition $\sigma'' > 0$, only bulk waves can propagate. This condition is satisfied for all ChP values (curves *1–5*).

WAVE FIELDS AND THE DISPERSION RELATION

In the examined waveguide structure, modes of the two types of linear polarization, TM and TE, can propagate. The components of the wave field of these modes depend on time and coordinates as follows:

$$F_\alpha(x,z,t) = F_\alpha(z)\exp[i(\omega t - \beta x)], \quad (2)$$

where $F_\alpha(z)$ are the profile functions, ω is frequency, and β is the complex propagation constant. For a wave of the TM type, the relationships between the compo-

nents of the field in each of the media ($j = 1, 2, 3$) are determined by the equations

$$\frac{\partial^2 H}{\partial z^2} - q_j^2 H_y = 0, \quad E_x = \frac{i}{k_0 \varepsilon_j} \frac{\partial H_y}{\partial z}, \quad E_z = -\frac{\beta}{k_0 \varepsilon_j} H_y. \tag{3}$$

Here, q_j are the transverse components of the wave vector in each of the media. In this case, $q_{1,3}^2 = \beta^2 - k_0^2 \varepsilon_{1,3}$, and $q_2^2 = k_0^2 \varepsilon_d - \beta^2$, where $k_0 = \omega/c$, and c is the speed of light in vacuum.

To solve the boundary problem, we will use the boundary conditions for the tangential components of the electric and magnetic fields of the mode,

$$E_{1x} = E_{2x}, \quad H_{1y} - H_{2y} = \frac{4\pi}{c}\sigma_1 E_{1x} \quad (z = 0),$$
$$E_{2x} = E_{3x}, \quad H_{2y} - H_{3y} = \frac{4\pi}{c}\sigma_2 E_{2x} \quad (z = d). \tag{4}$$

Equating the determinant of the system of the two pairs of Eqs. (4) to zero, we obtain the dispersion relation for the waves propagating in the structure:

$$q_d d = \pi m - \arctan\left(\frac{\varepsilon_1 q_d}{q_1 \varepsilon_d}\left(1 - \frac{4\pi\sigma_1}{c}\frac{q_1}{ik_0\varepsilon_1}\right)\right) - \arctan\left(\frac{\varepsilon_3 q_d}{q_3 \varepsilon_d}\left(1 - \frac{4\pi\sigma_2}{c}\frac{q_3}{ik_0\varepsilon_3}\right)\right). \tag{5}$$

This equation, in view of the complexity of its parameters, determines the relationship between the real and imaginary parts of the wavenumber $\beta = \beta' - i\beta''$ with the frequency of the electromagnetic wave. Here, Eq. (5) is written for the case of different conductivities at the waveguide boundaries and contains three different transverse components of the wave vector. In the approximation $\sigma_1 = \sigma_2 = 0$ (i.e., in the absence of graphene layers), expression (5) is reduced to the standard dispersion relation for a bulk mode in a dielectric waveguide [24].

NUMERICAL ANALYSIS

Below, we present the results of our numerical analysis of the regimes of waveguide propagation in the structure under consideration. In what follows, we will assume that the structure is in a vacuum; therefore, $\varepsilon_1 = \varepsilon_3 = 1$. The next two figures show the dispersion dependences for the waveguide modes in the examined structure, which are solutions of Eq. (5) and are presented as the dependences of the frequency on the normalized real part of propagation constant β'. Normalization was carried out to the quantity $k_T = k_B T/hc$, the value of which for the working temperature of $T = 300$ K was $k_T = 1314.24$ cm^{-1}. In Fig. 3a, these dependences were obtained for the first three waveguide modes with the numbers $m = 0$, 1, and 2 (curves *1–3*) at identical of the ChP of the graphene layers at both boundaries $\mu_1 = \mu_2 = 0.1$ and 0.2 eV (solid and dashed curves, respectively). It can be seen that, at the chosen fixed value of the propagation constant, a change in the ChP of the graphene layers from 0.2 to 0.1 eV, makes it possible to considerably extend the spectral range of occurrence of waveguide modes in the structure. Thus, at $\beta'/k_T = 400$, a similar change in the ChP leads to a more than twofold extension of the spectral interval of the first waveguide mode. Figure 3b shows the dispersion dependences for the dielectric layer thicknesses $d = 10$, 20, and 50 nm (curves *1–3*). It can be seen that, with an increase in the thickness of the dielectric film, the mode still exists in the entire spectral interval under consideration, but the range of propagation constants that correspond to fixed frequencies significantly narrows. Even at film thickness $d = 50$ nm (curve *3*), the dispersion law becomes almost linear.

In [17], the dispersion properties of the first TE modes in a rectangular waveguide with metal walls, dielectric filling, and a graphene layer have also been controlled by changing the ChP of graphene. It was also found that the transmission and reflection coefficients of the waveguide modes are influenced by the ChP. In this case, the distance from the graphene monolayer to the metal walls of the waveguide has an additional effect on the dispersion of the wave and waveguide characteristics.

Figure 4 shows the dispersion dependences for the first waveguide mode at different combinations of the ChP of graphene layers. Initially, we will consider a symmetric situation in which $\mu_1 = \mu_2 = 0.0$, 0.1, 0.2, and 0.3 eV (Fig. 4a, curves *1–4*). Our analysis shows that, in the considered spectral range $\omega = 10^{14}$–10^{15} s^{-1}, the first mode can propagate in the structure only if $\mu_1 = \mu_2 \le 0.3$ eV. In this case, the maximum value of the propagation constant is $\beta' \approx 600 k_T$, and it is achieved at $\mu_1 = \mu_2 = 0.1$ eV, which corresponds to a smallest value of the mean free path of the wave for the chosen values of the parameters. As the ChP of the graphene coatings increases, the range of existence of the first mode shifts to higher frequencies, and the range of possible propagation constants narrows; i.e., the interval of the path lengths of the mode at a fixed frequency value narrows. Thus, for $\mu_1 = \mu_2 = 0.5$ eV, waveguide modes can exist in the frequency range $\omega = (1.6–2.0) \times 10^{15}$ s^{-1}. In this case, the maximum value of their propagation constant decreases to $\beta'/k_T \approx 23$, which corresponds to an increase in the free path of the wave for the chosen values of the parameters.

In an asymmetrical situation, in which the ChP changes only for one of the graphene layers, for example, $\mu_1 = 0.1$ eV, while $\mu_2 = 0.0$, 0.2, and 0.3 eV (Fig. 4b, curves *1*, *3*, and *4*), the dispersion relations acquire a more complicated form. It can be seen that

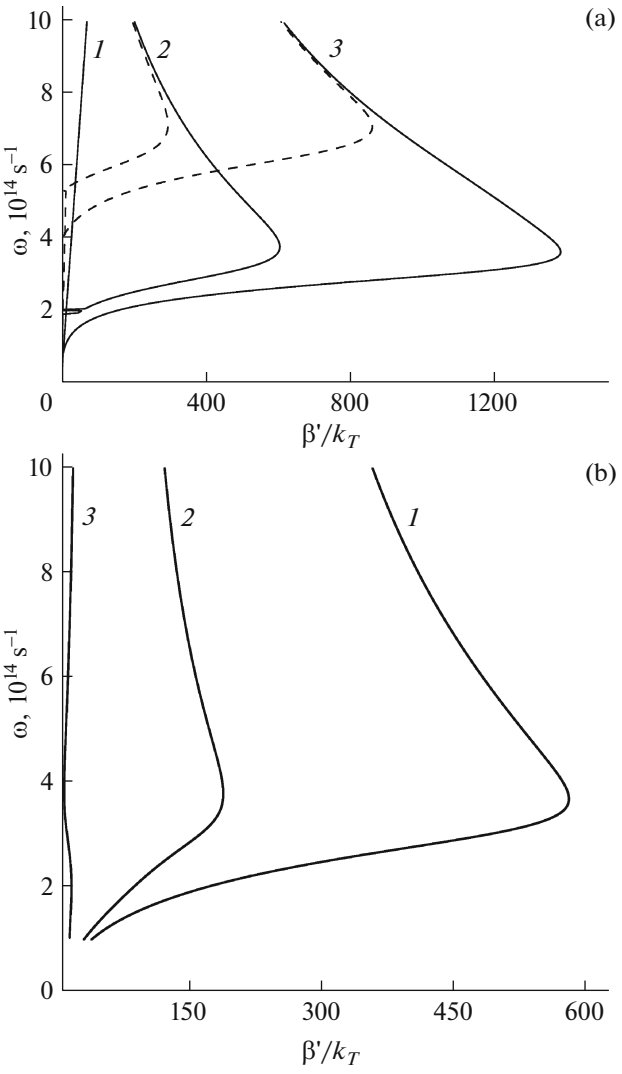

Fig. 3. Frequency dependences for waveguide modes with $m = 0$, 1, and 2 ((a), curves *1–3*) at $\mu_1 = \mu_2 = 0.1$ and 0.2 eV (solid and dashed curves, respectively); (b) frequency dependences for the first mode at $\mu_1 = \mu_2 = 0.1$ eV and $d =$ 10, 20, and 50 nm (curves *1–3*).

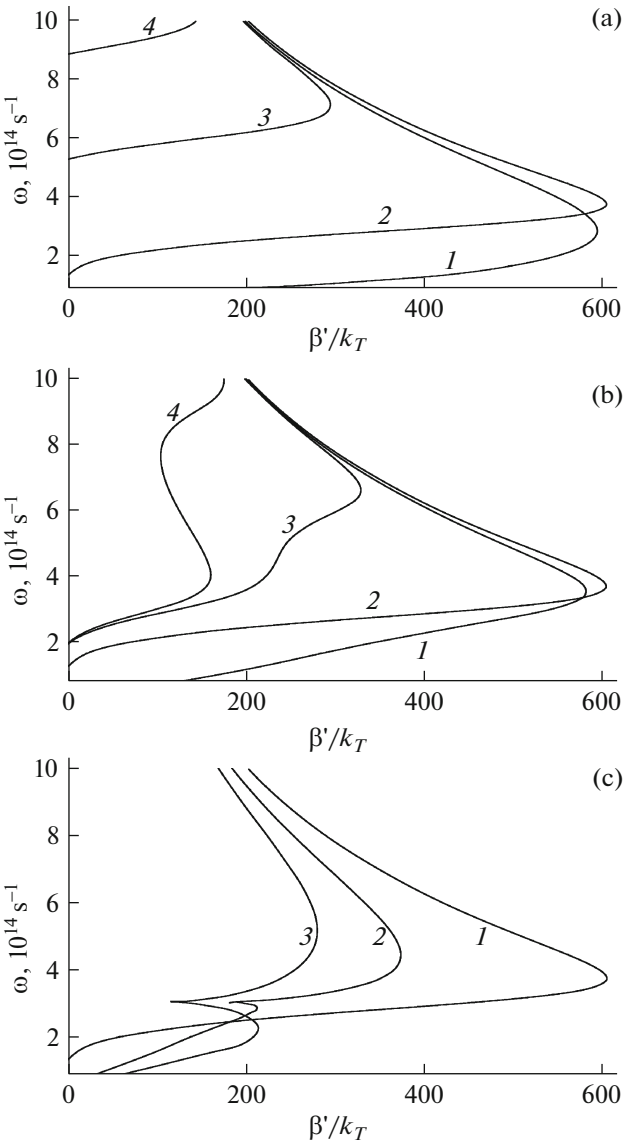

Fig. 4. Frequency dependences for the first mode with (a) $\mu_1 = \mu_2 = 0$, 0.1, 0.2, and 0.3 eV (curves *1–4*); (b) $\mu_1 =$ 0.1 eV and $\mu_2 = 0$, 0.1, 0.2, and 0.3 eV (curves *1–4*); and (c) $\mu_1 = 0.1$ eV and $\mu_2 = 0.1$ and –0.1 eV (curves *1, 2*) and $\mu_1 = \mu_2 = -0.1$ eV (curve *3*).

the greater the difference between the ChP of the layers, the greater is the degree to which the character of the dispersion of the waveguide modes changes, and peculiarities associated with the presence of graphene begin to appear: in particular, the range of their existence also narrows, but additional extrema of dependence $\beta'(\omega)$ appear, which correspond to an infinitely large group velocity. Moreover, by varying the values of the ChP of graphene layers, it is possible to shift the frequency range in which the group velocity of waves is negative. At negative values of the ChP on one of the coatings, bends appear on the dispersion dependences as a result of the occurrence of a resonance of the imaginary part of the graphene conductivity: $\mu_1 =$ 0.1 eV, $\mu_2 = 0.1$ and –0.1 eV (Fig. 4c, curves *1, 2*). The effect becomes more pronounced when the values of the ChP of the graphene layers are negative: $\mu_1 = \mu_2 =$ –0.1 eV (curve *3*).

Figure 5 shows the distributions of the electric and magnetic fields of the first mode ($m = 1$) over the cross section of the structure that correspond to the frequency $\omega = 4 \times 10^{14}$ s^{-1} and different ChP values μ_1 and μ_2. The distributions were plotted for the two cases in which (i) $\mu_1 = \mu_2 = -0.1$, 0.0, and 0.1 eV (dashed, solid, and dotted curves, respectively, in Fig. 5a) and (ii) $\mu_1 = 0$, 0.1, and 0.3 eV, while $\mu_2 = 0.1$ eV (dashed, solid, and dotted curves, respectively, in Fig. 5b). It is

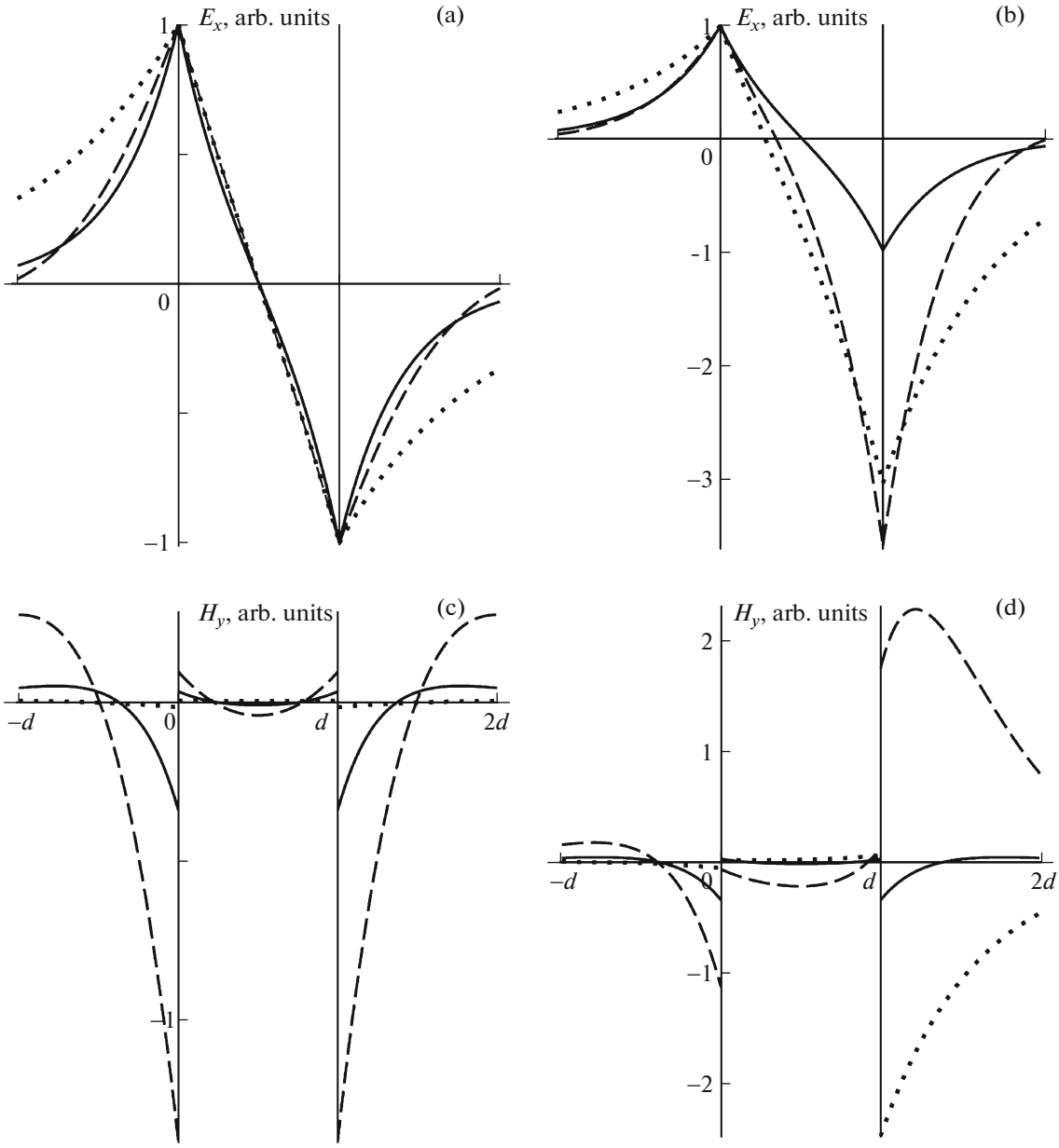

Fig. 5. Distributions of the electric and magnetic fields over the structure for the first waveguide mode at (a) $\mu_1 = \mu_2 = -0.1$, 0.0, and 0.1 eV (dashed, dotted, and solid curves, respectively) and (b) $\mu_1 = 0$, 0.1, and 0.3 eV and $\mu_2 = 0.1$ eV (dashed, solid, and dotted curves, respectively); $\omega = 6 \times 10^{14}$ s^{-1}.

seen that the occurrence of graphene monolayers leads to a discontinuity of the magnetic field at the boundaries of the waveguide layer. At symmetric values of the ChP, the distributions of the fields in the waveguide structure also are symmetric. This figure also shows the case of an antisymmetric electric field and a symmetric magnetic field. At $\mu_1 \neq \mu_2$, the symmetry in the distribution of the fields disappears. By changing the value of the ChP, one can significantly modify the distribution of the wave field in the structure, thereby affecting its dispersion properties.

Further, based on the above dispersion dependences, we considered the influence of graphene coatings on the frequency dependences of the phase (Fig. 6) and group (Fig. 7) velocities for the first waveguide mode. These dependences were plotted using the following values of the ChP: (i) $\mu_1 = \mu_2 = -0.1$, 0.1, 0.2, and 0.3 eV (Figs. 6a, 7a, curves *1*–*4*) and (ii) $\mu_1 =$ 0.1 eV, while $\mu_2 = -0.1$, 0.1, 0.2, and 0.3 eV (Figs. 6b, 7b, curves *1*–*4*). For phase velocity $v_{ph} = \omega/\beta'$, after its sharp fall in a narrow spectral range, a subsequent smooth growth of this quantity is observed, which is

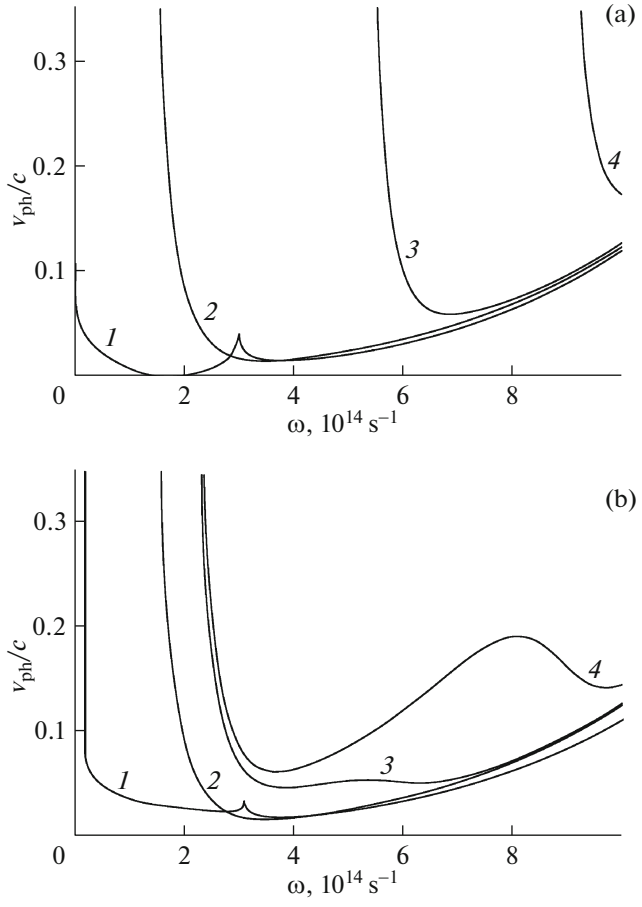

Fig. 6. Frequency dependences of the phase velocity for the first waveguide mode at (a) $\mu_1 = \mu_2 = -0.1$, 0.1, 0.2, and 0.3 eV (curves *1–4*) and (b) $\mu_1 = 0.1$ eV and $\mu_2 = -0.1$, 0.1, 0.2, and 0.3 eV (curves *1–4*).

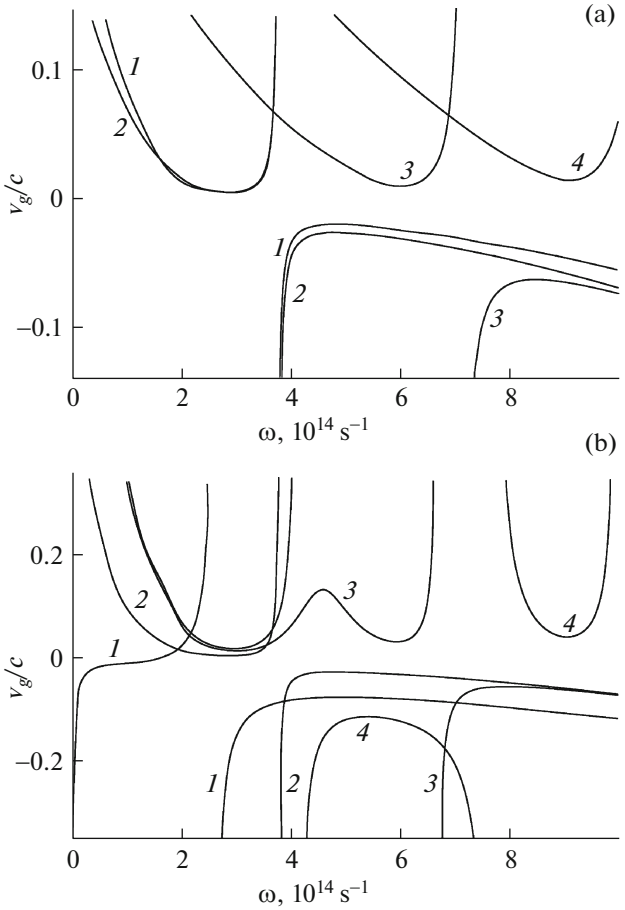

Fig. 7. Frequency dependences of the group velocity for the first waveguide mode at (a) $\mu_1 = \mu_2 = -0.1$, 0.1, 0.2, and 0.3 eV (curves *1–4*) and (b) $\mu_1 = 0.1$ eV and $\mu_2 = -0.1$, 0.1, 0.2, and 0.3 eV (curves *1–4*).

characteristic of the ChP values $\mu_1 = \mu_2 = 0.1$ and 0.2 eV (Fig. 6a, curves *2*, *3*). Minimum values that the phase velocity of the wave can reach in the structure are $v_{ph}/c \simeq 0.02$ (i.e., a 50-fold slowing-down), and they correspond to a zero ChP (curve *1*). From the point of view of the wave slowing-down, the choice of the zero ChP is optimal, at which v_{ph} can be considered to be small and constant in the range $\omega = (1–3) \times 10^{14}$ s^{-1}. If the values of the ChP at the waveguide boundaries are different, the function $v_{ph}(\omega)$ may have one or several extrema (Fig. 6b, curves *3*, *4*), which opens up additional possibilities for controlling. We note that, compared to the case in which the values of the ChP of the coatings are equal to each other and the ranges of observation of the waves narrow with a simultaneous increase in the ChP, if the ChP of the upper boundary is fixed, while that of the lower boundary varies, no narrowing of the range of existence of the waves takes place (Fig. 6b, curves *2–4*).

The slowing-down of the first waveguide modes in the structure formed by a dielectric waveguide, a graphene monolayer, and a covering medium has also been established in [18]. Thus, in the mid-IR range (8–16 μm), the values of the mode effective refractive index reached values close to 100. This indicates that the phase velocities of waves propagating in the structure can be almost two orders of magnitude lower than the speed of light in a vacuum.

Group velocity $v_g = d\omega/d\beta'$, up to the critical frequency, which corresponds to the inflection of the dispersion curve (and, as a result, to the tendency to infinity $v_g \to \infty$), is characterized by positive values. For waves with frequencies $\omega > \omega_{cr}$, the group velocity is negative. The frequency range, in which the group velocity is negative, can be shifted due to a change of the ChP of the lower coating (Fig. 7a, curves *1–4*). At the values of the ChP $\mu_1 = 0.1$ eV and $\mu_2 = 0.2$ eV, the group velocity acquires small and positive values in the frequency range $\omega = (1.0–3.5) \times 10^{14}$ s^{-1} (Fig. 7b, curve *3*). For negative values of the ChP, an additional

frequency range appears in which a negative group velocity of the waveguide mode is observed (curves *2*, *3*).

CONCLUSIONS

In this paper, we considered particular features of the propagation of first waveguide modes in a dielectric layer that was placed between two graphene monolayers. The ChP of graphene can be varied by changing the gate voltage between the graphene coatings. We showed that the dispersion parameters of the first waveguide mode can be controlled by changing the ChP of the graphene layers. In particular, one can control the range of existence of the waveguide mode, its phase and group velocities. The examined waveguide structure can be used as a basis for compact dielectric waveguiding structures, the dispersion characteristics of which can be rearranged by an external electric field in the process of propagation of modes.

ACKNOWLEDGMENTS

This work was supported by the Russian Science Foundation (project no. 17-72-10135) and by the Ministry of Education and Science of the Russian Federation (project no. 14.Z50.31.0015).

REFERENCES

1. I. V. Iorsh, I. V. Sharidov, P. A. Belov, and Yu. S. Kivshar, JETP Lett. **97**, 287 (2013). doi 10.7868/S0370274X13050020
2. D. Yu. Fedyanin, A. V. Arsenin, V. G. Leiman, and A. D. Gladun, Quantum Electron. **39**, 745 (2009). doi 10.1070/QE2009v039n08ABEH014072
3. I. Suarez, A. Fernando, J. Marques-Hueso, A. Diez, R. Abarguez, P. Rodriguez-Canto, and J. Martinez-Pastor, Nanophoton. **6**, 1109 (2017). doi 10.1515/nanoph-2016-0166
4. V. M. Agranovich and D. L. Mills, *Surface Polaritons: Electromagnetic Waves at Surfaces and Interfaces* (Elsevier Science, Amsterdam, 1982).
5. N. R. Fong, M. Menotti, E. Lisicka-Skrzek, H. Northfield, A. Olivieri, N. Tait, M. Liscidini, and P. Berini, ACS Photon. **4**, 593 (2017). doi 10.1021/acsphotonics.6b00930
6. P. Berini and I. de Leon, Nat. Photon. **6**, 16 (2012). doi 10.1038/nphoton.2011.285
7. E. Verhagen, J. A. Dionne, L. Kuipers, and A. Polman, Nano Lett. **8**, 2925 (2008). doi 10.1021/nl801781g
8. D. N. Basov and T. Timusk, Rev. Mod. Phys. **77**, 721 (2005). doi 10.1103/RevModPhys.77.721
9. N. Kaina, A. Causier, Y. Bourlier, M. Fink, T. Berthelot, and G. Lerosey, Sci. Rep. **7**, 15105 (2017). doi 10.1038/s41598-017-15403-8
10. S. A. Gad, M. Boshta, A. M. Moustafa, and A. M. Abo El-Soud, Solid State Sci. **13**, 23 (2011). doi 10.1016/j.solidstatesciences.2010.09.022
11. D. A. Smirnova, I. V. Iorsh, I. V. Sharidov, and Yu. S. Kivshar, JETP Lett. **99**, 527 (2014). doi 10.1134/S002136401408013X
12. E. Hajaj, O. Shtempluk, V. Kochetkov, A. Razin, and Y. Yaish, Phys. Rev. B **88**, 045128 (2013). doi 10.1103/PhysRevB.88.045128
13. D. A. Evseev, S. V. Eliseeva, and D. I. Sementsov, Eur. Phys. J. Appl. Phys. **80**, 10501 (2017). doi 10.1051/epjap/2017170167
14. D. A. Evseev and D. I. Sementsov, Opt. Spectrosc. **124**, 230 (2018). doi 10.21883/OS.2018.02.45530.129-17
15. L. Wang, Q. Yan, H. Xu, H. Wang, G. Zhang, and X. Zhou, Phys. Lett. A **380**, 3297 (2016). doi 10.1016/j.physleta.2016.07.063
16. A. Gorbach, A. Marini, H. Alkorre, and D. Skryabin, Opt. Lett. **38**, 5244 (2013). doi 10.1364/OL.38.005244
17. G. Shkerdin, H. Guo-Qiang, H. Alkorre, and J. Stiens, J. Opt. **19**, 015606 (2017). doi 10.1088/2040-8986/19/1/015606
18. W. Xu, Z. Zhu, K. Liu, J. Zhang, X. Yuan, Q. Lu, and S. Qin, Opt. Express **23**, 5147 (2015). doi 10.1364/OE.23.005147
19. C. H. Gan, H. S. Chu, and E. P. Li, Phys. Rev. B **85**, 125431 (2012). doi 10.1103/PhysRevB.85.125431
20. L. A. Falkovsky, Phys. Usp. **55**, 1140 (2012). doi 10.3367/ UFNe.0182.201211i.1223
21. G. W. Hanson, J. Appl. Phys. **103**, 064302 (2008). doi 10.1063/1.2891452
22. K. S. Novoselov, A. K. Geim, S. V. Morozov, D. Jiang, Y. Zhang, S. V. Dubonos, I. V. Grigorieva, and A. A. Firsov, Science (Washington, DC, U. S.). **306**, 666 (2004). doi 10.1126/science.1102896
23. Z. Z. Alisultanov and R. P. Meilanov, Semiconductors **48**, 924 (2014). doi 10.1134/S1063782614070021
24. M. S. Sodha and A. K. Ghatak, *Inhomogeneous Optical Waveguides* (Plenum, New York, 1977).

Translated by V. Rogovoi